Molecular Therapy
Nucleic Acids
Original Article

CRISPR-Cas9-mediated reactivation of the uricase pseudogene in human cells prevents acute hyperuricemia

Lais de Lima Balico[1] and Eric A. Gaucher[1]

[1]Department of Biology, Georgia State University, 100 Piedmont Ave., Atlanta, GA, 30303, USA

The utility of CRISPR-Cas9 to repair or reverse diseased states that arise from recent genetic mutations in the human genome is now widely appreciated. The use of CRISPR to "design" the outcomes of biology is challenged by both specialized ethicists and the general public. Less of a focus, however, is the ability of CRISPR to provide metabolic supplements or prophylactic molecules that improve long-term human health by overwriting ancient evolutionary events. Here, we use CRISPR to genomically integrate a functional uricase gene that encodes an enzymatically active protein into the human genome. These uricase-producing cells are able to reduce or even eliminate high concentrations of exogenous uric acid despite the enzyme being localized to peroxisomes. Our evolutionary engineered cells represent the first instance of the primate ape lineage expressing a functional uricase encoded in the genome within the last 20 million years. We anticipate that human cells expressing uricase will help prevent hyperuricemia (including gout) as well as hypertension and will help protect against fatty liver disease in the future.

INTRODUCTION

Uric acid is a highly insoluble metabolic product of purine metabolism generated from the breakdown of nucleic acids. In most species, uric acid (in the form of monosodium urate) is metabolized to 5-hydroxyisourate by the enzyme uricase (urate oxidase), with hydrogen peroxide as a by-product. Depending on the species, 5-hydroxyisourate is metabolized to allantoin and then further degraded to generate ammonia/urea and excreted from the body. Uric acid is recognized as an antioxidant and considered to be one of the most important antioxidants in the plasma,[1] although its role in oxidative stress has recently been disputed.[2] Most animals have a functional uricase enzyme and have serum uric acid levels in the 1–2 mg/dL range (60 to 120 μM). In contrast, serum uric acid levels are higher in the Lesser and Great Apes (including humans) because of parallel nonsense mutations that caused a pseudogenization of the uricase gene via premature stop codons thought to have occurred during the mid-Miocene (~20 million years ago, Ma).[3]

It has been hypothesized that the loss of an active uricase in lineages leading to apes was contemporaneous with an increase in the concentration of uric acid in the serum of ancestral apes and may have been advantageous.[4–9] Nevertheless, it is clear that the concentrations of uric acid are higher in human serums (3–7 mg/dL for men and 2–6 mg/dL for women) than in closely related primates that have a functional uricase (0.4–0.8 mg/dL in some Old World Monkeys).

The higher concentration of uric acid in humans is associated with clinical diseases. High levels of uric acid (hyperuricemia) are classically associated with gout—where uric acid crystallizes in the tissues. These needle-shaped monosodium urate crystals are deposited in avascular tissues (e.g., cartilage, tendons, ligaments). In severe cases, these crystals are deposited in larger central joints and in the parenchyma of organs such as the kidney.

Uric acid has also been recognized as a predictive marker for cardiovascular disease, hypertension, and renal disease.[8] Hyperuricemia occurs in 25%–50% of hypertensive patients and in up to 90% of those with new-onset hypertension.[10] Some studies suggest that high levels of uric acid confer a risk equivalent to the risk cholesterol poses for cardiovascular events. Hyperuricemia is also a reported risk factor for the progression of renal disease; over 95% of patients with gout have interstitial renal disease at autopsy.[11]

Uric acid levels can be managed at various points in the urate metabolic pathway. Gertrude Elion and George Hitchings won the Nobel Prize in 1988 for their treatment of hyperuricemia using allopurinol. This small molecule inhibits xanthine oxidoreductase activity and thus manages the production of uric acid but is unfortunately not able to reduce urate concentration to safe levels (6 mg/dL) for ~40% of gout suffers.[12] At the protein level, recombinant active uricases have been injected into human patients in order to oxidize uric acid. A therapeutic uricase was first available to patients as purified endogenous or recombinantly expressed uricase from the fungus *Aspergillus flavus* (uricozyme and rasburicase/ELITEK, respectively). Although active in the metabolism of uric acid to 5-hydroxyisourate, these enzymes are highly antigenic, and repeated administration results in allergic reactions, anaphylaxis, and sometimes death due to

Received 5 May 2021; accepted 9 August 2021;
https://doi.org/10.1016/j.omtn.2021.08.002.

Correspondence: Eric A. Gaucher, Department of Biology, Georgia State University, 100 Piedmont Ave., Atlanta, GA 30303, USA.
E-mail: egaucher@gsu.edu

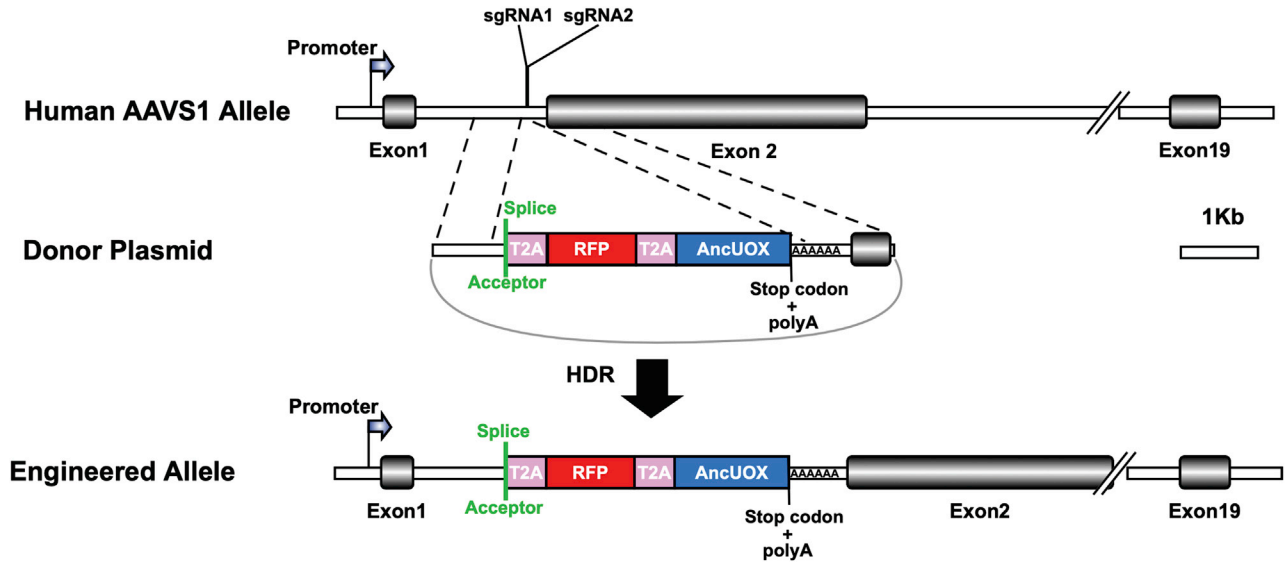

Figure 1. Schematic for CRISPR-Cas9-mediated knockin of exogenous DNA fragment into human *AAVS1* locus in HEK293 cells

Top: the human *AAVS1* allele. gRNA sequences are designated (g1 and g2) and located upstream of exon 2. Center: donor plasmid is represented schematically. Dashed lines show homology arms (~800 bp on each side of donor) between genomic locus and plasmid DNA. A splice acceptor sequence is inserted upstream of RFP gene to allow proper RNA splicing using the endogenous transcriptional promoter. T2A sequences are inserted both upstream and between RFP/AncUOX to allow the release of the individual proteins after translation. SV40 poly(A) signal sequence is designated downstream of the donor DNA. Bottom: engineered allele. Post Cas9 cuts at the site corresponding to the gRNA sequences, donor DNA is integrated into the breakpoint through homology directed repair (HDR).

antibody development against uricase epitopes.[13] As such, these therapeutics are designated with black box warnings and only administered a couple of times in patients to prevent tumor lysis syndrome (accumulation of uric acid crystals in the kidneys due to the release of massive amounts of purine nucleic acid from lysed tumor cells during cancer treatments). The most recent FDA-approved uricase is a polyethylene glycol (PEGylated)-modified form of a pig-baboon chimeric uricase (pegloticase or KRYSTEXXA). KRYSTEXXA has shortcomings, however, in both its safety and efficacy. In phase III clinical studies, 18% of patients discontinued treatment in response to serious adverse events. Furthermore, <50% of patients met defined endpoints in lowering blood serum uric acid levels and resolution of gouty tophi.[14,15] A more recent study shows that 40% of patients in clinical trials develop high-titer antibodies to the PEG moiety of KRYSTEXXA and 14% develop antibodies to uricase epitopes, and that in total these antibodies compromise the utility of the therapeutic.[16] Thus, KRYSTEXXA is currently being reformulated with a different PEG moiety by 3SBio.

More recent innovation around uricase delivery to human patients involves the use of enzymosomes and nanozymes.[17,18] These nano-sized vesicles entrap both uricase and catalase (or catalase-like materials), and their advantage is 2-fold: (1) minimize the human immune response by shielding the foreign uricase and (2) minimize the amount of hydrogen peroxide by-product via neutralization. The latter goal is particularly important since hydrogen peroxide has a toxic effect on tissues[19] and it preferentially reacts with the heme co-factor from hemoglobin when present in blood.

We previously demonstrated that human uricase can be reactivated by replacing the two premature stop codons, as well as replacing a number of sense mutations that caused amino acid replacements that greatly diminished enzyme activity during uricase evolution.[4] The ability to genomically integrate this uricase into human cells would improve our basic understanding of uric acid's effect on human metabolism and also help develop novel therapeutics that both prevent and treat hyperuricemia.

RESULTS

As a first step to generate genomically engineered human cells containing an active uricase gene, we evaluated the efficiency of insert donor DNA into human *AAVS1* safe harbor locus with a CRISPR-Cas9-mediated system.[20] *AAVS1* permits robust expression of transgenes in the *PPP1R12C* locus without noticeable phenotypic impairments.[21]

We generated a CRISPR plasmid by replacing the *mCherry* gene (Addgene #64222) with a *GFP* gene, and we then cloned two separate gRNA sequences based on the published literature that target the human *AAVS1* locus.[22] The CRISPR plasmid was designed to generate gRNA, Cas9 protein, GFP (to visually confirm plasmid transfection), and the adenovirus 4 E4orf6 (Ad4E4orf6) protein. The latter protein mediates the ubiquitination and proteosomal degradation of DNA ligase IV and consequently inhibits non-homologous end joining (NHEJ) repair and thus promotes homology directed repair (HDR) from a donor plasmid.[22–24] A donor plasmid was assembled to carry flanking homology arms that allow homologous recombination (~800 bp, Figure 1) and contained the *RFP* gene (for downstream

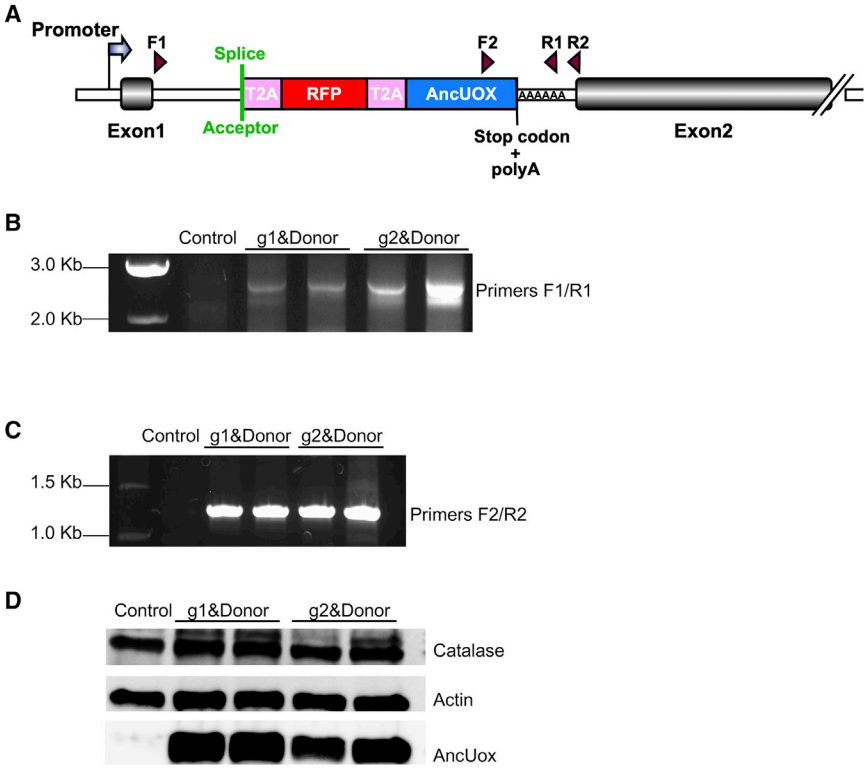

Figure 2. Knockin of exogenous DNA fragment into human *AAVS1* locus validation

(A) Schematic of engineered allele is shown. Positions of PCR primers used for detection of donor insertion are shown. (B) Genomic PCR detection of the donor integration. Primer pair F1/R1 amplified one fragment that represented target allele (2,863 bp). (C) PCR analysis of the donor integration. Primer pair F2/R2 detected one fragment that represented donor integration (1,201 bp). All genomic PCR analyses showed DNA fragments at their expected bp sizes in cells transfected with both CRISPR vector and donor plasmid. (D). Western blot analysis of whole lysates from HEK293 cells demonstrates the expression of AncUOX (~35 kDa). Actin and catalase were used as positive controls.

fluorescence-activated cell sorting [FACS]) and the ancestral *uricase* gene (AncUOX) separated by the self-cleaving protein domain T2A. When a double-stranded break induced by the Cas9 protein is successful, repair via HDR can occur with the donor plasmid being inserted into *AAVS1* locus and subsequent expression of RFP and AncUOX. The RFP expression allows direct screening by FACS. Transfections were performed in two independent experiments. Seventy-two hours after transfection we detected GFP signal, indicating positive expression of the CRISPR plasmid. RFP signal was subsequently visualized, and after two passages cells were screened by FACS. The RFP-positive (RFP^+) cells were isolated from non-transfected cells for further culturing.

To determine the correct integration of donor plasmid, we performed genotyping by PCR and DNA sequencing (data not shown) of both RFP^+ and control cells. Figure 2A shows a schematic of our engineered allele along with primer sites. The PCR analysis using primers that anneal immediately upstream of the 5′ homology arm and the 3′ end of the donor insert (at the polyA tract, immediately upstream of the 3′ homology arm) confirmed the precise genomic insertion of the donor sequence (Figure 2B). Additionally, a separate PCR reaction showed that the donor was correctly integrated at the *AAVS1* locus; in this reaction we used a set of primers that bind to the *AncUOX* gene immediately downstream of the 3′ homology arm (Figure 2C). PCR reactions were submitted for sequencing (results not shown). Sequencing analysis confirmed the correct junction between regions upstream and downstream of the insert into the *AAVS1* locus. We did not identify any new point mutations in the donor open reading frame (ORF) post-insertion into the genome.

To examine whether the new AAVS1 ORF was able to express the *AncUOX* gene, we performed western blot analysis from the whole lysate of control wild-type and RFP^+ cells. Western blot analysis confirmed AncUOX expression at the expected size (~35 kDa) only in RFP^+ cells; control cells did not show uricase expression. Catalase and actin proteins were used as loading controls, and both proteins were identified in all samples (Figure 2D).

To investigate whether AncUOX was located within peroxisomes, we performed immunofluorescent colocalization analyses. Cells were stained with antibodies specific to either the peroxisomal membrane (PMP70) or uricase (AncUOX). Image overlays demonstrated that AncUOX is appropriately colocalized to peroxisomes in HEK293 cells (Figure 3, yellow).

To evaluate the enzymatic activity of AncUOX after HDR-mediated integration, we utilized spectrophotometry to determine the oxidation of uric acid by following absorbance at 293 nm (decrease in absorbance indicates oxidation of the uric acid substrate). Uricase activity was confirmed in cells containing correctly integrated donor sequence but not in control cells (Figure 4). The analysis confirmed that AncUOX was able to completely oxidize uric acid when exposed to 100 and 200 μM exogenous uric acid. These cells also appear to eliminate endogenous uric acids, since substrate levels eventually flatten below the initial baseline. The addition of 400 μM uric acid (moderate hyperuricemia, ~6 mg/dL) demonstrated that AncUOX oxidizes at least all of the exogenous uric acid but the substrate levels return only to baseline (they do not proceed below baseline). To model severe hyperuricemia (~10 mg/dL) in human cells, we exposed cells to 600 μM uric acid. AncUOX was able to decrease uric acid, but the values did not return back to baseline as seen at other substrate concentrations. The uricase enzyme suffers from product inhibition,

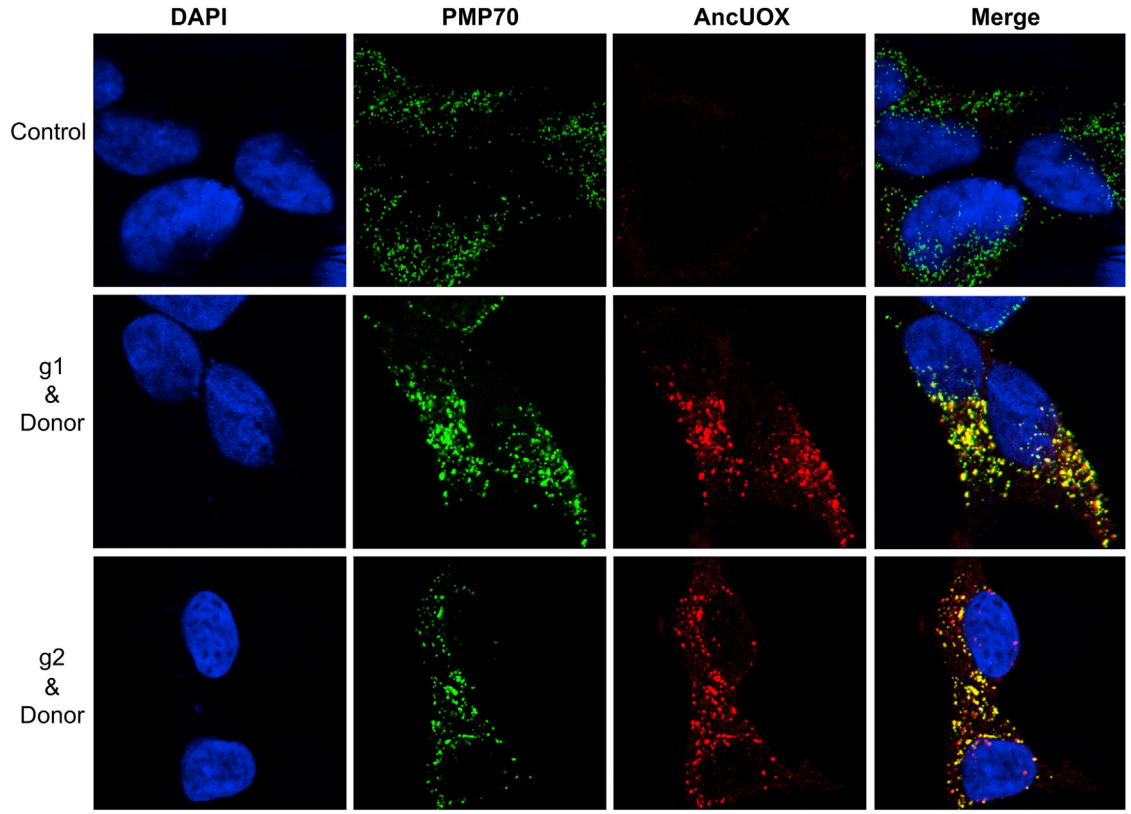

Figure 3. Immunofluorescent colocalization analysis between AncUOX and peroxisomes

Representative images of nuclei stained with DAPI (blue), PMP70 (peroxisome-specific marker, green) and AncUOX (red). Merged images demonstrate colocalization (yellow) after integration and expression of donor DNA into *AAVS1* locus.

which may explain why cells exposed to high concentrations (400 and 600 μM) could not achieve pre-exposure levels even after 2 h (complete data not shown). In total, AncUOX demonstrated activity against various uric acid concentrations and confirmed that AncUOX expression can help manage hyperuricemia.

DISCUSSION

The biomedical community has a complicated history with the development of recombinant uricases. The discovery that humans do not synthesize their own active enzyme, and are thus susceptible to the buildup of uric acid, has necessitated innovation around uricase delivery to human patients. Therapeutic uricases were initially developed based on purified enzymes from *Aspergillus* fungi and porcine, as well as their recombinant versions expressed in the laboratory. Other uricases have focused on the enzyme from baboon, other mold/yeast, various bacteria, and canine and completely synthetic versions that attempt to optimize stability and activity for delivery to humans. Even the delivery methods and formulations themselves have necessitated innovation. These include intravenous and subcutaneous injections, topical ointments, nano-carriers, PEGylation and other protective carbohydrate moieties, co-administration with immune suppressors, and oral delivery via modified *Staphylococcus*, among others. One current human clinical trial consists of a engineered *Candida* yeast uricase by Allena Pharmaceuticals for oral delivery with enhanced gastrointestinal stability to manage serum uric acid levels via control of purine metabolism in the large intestine.[25] There is clearly a lot of competition for a share of the gout/hyperuricemia market using an active uricase enzyme.

A genomic engineering approach that reintroduces an active uricase to human cells potentially circumvents many of the barriers that hinder most developments of a uricase therapeutic. Our genomically integrated uricase encodes the conserved 3-amino acid peroxisomal signal (S-K-L) that is accessible on the carboxyl terminus to allow uptake of the uricase by peroxisomes. The colocalization of our recombinant uricase along with endogenous catalase in the peroxisomes ensures that hydrogen peroxide generated from the oxidation of uric acid is neutralized within the organelle and thus prevents any toxic effects of hydrogen peroxide with tissues or blood. The peroxisomal localization of our uricase may also preclude a severe immune response since (1) the peroxisomes are protected against antibodies and (2) our uricase does not require PEG moieties for stabilization like other recombinant uricases.

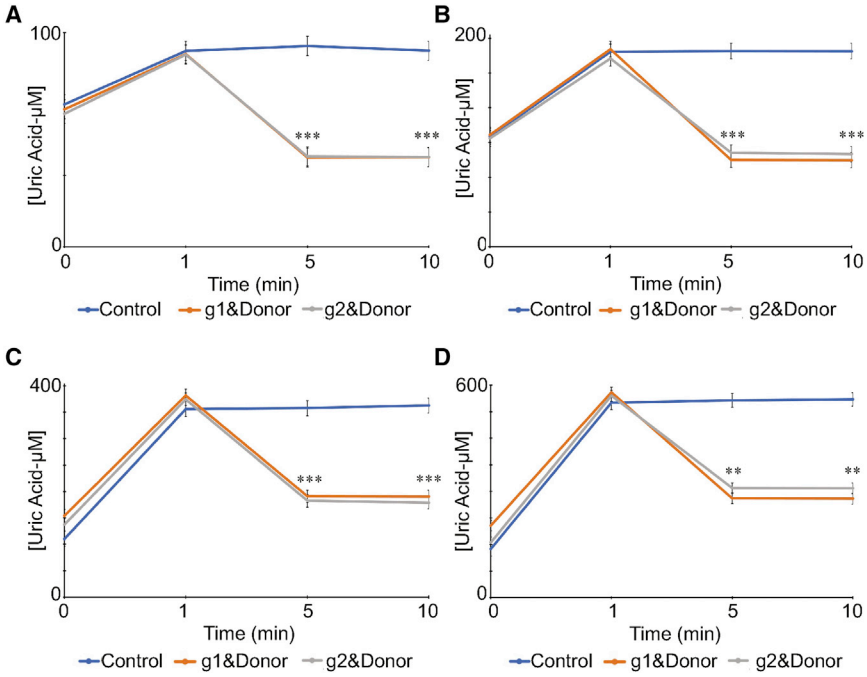

Figure 4. Intracellular uricase activity

Uricase activity was monitored by the oxidation of uric acid. (A) 100 μM uric acid. (B) 200 μM uric acid. (C) 400 μM uric acid. (D) 600 μM uric acid. Cells expressing AncUOX show a decrease of absorbance at 293 nm (indicative of uricase activity) in all assayed conditions. Results are displayed as mean ± SEM from three replicate assays. ***$p < 0.05$ and **$p < 0.01$ versus controls. Data were normalized by total protein concentration.

We have demonstrated that CRISPR-Cas9 can be used to genomically integrate a functional uricase into human kidney cells. Kidney cells from non-ape mammals are known to moderately express uricase and oxidize uric acid.[26,27] Our engineered cells may lead to novel therapeutics in the future to manage chronic kidney disease in the face of hyperuricemia.[28] A further extension of our system can also be applied to liver cells. We are particularly interested in understanding the potential role of uricase in limiting fructose's ability to stimulate fat synthesis in the liver (most fat in humans is synthesized in the liver and adipose tissue); thus we intend to utilize our uricase genome engineering system in human liver cells. We could then assay for the broad-scale effects that uricase expression has on fat synthesis and fat metabolism in hepatocytes.

NIH Director Francis Collins announced in 2019 that advances in organoid development are beginning to have a profound effect on our understanding of fatty liver disease (NIH Director's Blog, June). Liver-like organoids are capable of producing hepatocytes.[29–31] This has 2-fold importance for us: (1) uricases are highly expressed in these cells (in non-ape mammals), and (2) fat can accumulate in these organoid cells when exposed to fatty acids. Since we have experimentally shown that transient uricase expression in human liver cells significantly inhibits fatty acid synthesis,[4] it should be worth growing liver-like organoids stably expressing a functional uricase to explore whether this can prohibit fat accumulation over longer periods of time, especially when exposed to fructose. These cell lines would also allow us to more thoroughly interrogate the biochemical mechanisms of uric acid on cellular metabolism, and allow us to use these engineered cells to develop organoids to study fatty liver disease and potentially engineered patient cells to introduce a functional uricase enzyme to combat liver malfunction as an alternative to organ transplant.[29–31]

In total, our results demonstrate for the first time that HDR-mediated donor integration of recombinant uricase into human cells can be highly specific and efficient, and that expression of active uricase can be used for gene therapy to potentially treat/prevent hyperuricemia in human patients and as a general prophylactic to manage healthy levels of uric acid. We have also extended the biomedical utility of ancient proteins to treat/prevent diseases.[32–35] We further anticipate that future studies will provide more insights into the advantages and/or disadvantages of uric acid's role as a critical antioxidant and its connection to the loss of vitamin C synthesis in the Haplorhini clade of mammals (tarsiers, monkeys, and apes).[5,6,8,36,37]

MATERIALS AND METHODS

Cell culture

Human embryonic kidney cells (HEK293) were purchased from ATCC. HEK293 cells were cultured in Dulbecco's modified Eagle's medium (DMEM, Corning) supplemented with 10% fetal bovine serum (FBS, Corning) and 1% antibiotic-antimycotic solution (Gibco). Cells were passaged approximately three times per week and maintained in a humidified incubator at 37°C with 5% CO_2.

Construction of CRISPR and donor plasmids

To construct the pU6-(Bbs1)_CBh-Cas9-T2A-GFP-p2A-Ad4E4orf6 plasmid (CRISPR plasmid), we digested px458 (Addgene, #48138) and pU6-(BbsI)_CBh-Cas9-T2A-mCherry-P2A-Ad4E4orf6 (Addgene, #64222) with FseI/BsrGI (New England Biolabs). The GFP fragment was ligated into pU6-(BbsI)_CBh-Cas9-T2A-_-P2A-Ad4E4orf6 vector from which the RFP/mCherry gene was removed. *AAVS1* target sequences of gRNA used in our study were previously published (Table S1).[22] gRNA oligonucleotides were annealed and cloned into BbsI sites to generate both the gRNA1-CRISPR and gRNA2-CRISPR plasmids.[38]

To generate the AAVS1-SA-T2A-RFP-T2A-AncUOX-SV40polyA-signal donor plasmid, the coding regions for RFP-T2A-AncUOX-SV40polyAsignal were synthesized as mammalian codon-optimized

sequences by GenScript (Thermo Scientific), amplified, and cloned into AAVS1 SA-T2A-puro pA donor (Addgene #22075) by Gibson Assembly (New England Biolabs). Primers used are listed in Table S1.

Transfection and fluorescence-activated cell sorting

HEK293 were transfected with TransfeX Reagent (ATCC) according to the manufacturer's protocol. Briefly, 24 h prior to transfection, 1×10^6 cells were plated into a single well of a 6-well plate. For each transfection, 2 μg of gRNA1- or gRNA2-CRISPR plasmid was mixed with 4 μg of donor plasmid in Opti-MEM (Invitrogen) and 12 μL of TransfeX. After 15 min of incubation at room temperature, DNA complexes were mixed carefully into the wells containing the cells. Transfected cells were passaged at least twice before FACS. Bulk cell sorting was performed on a BD FACS Aria II (BD Biosciences); the RFP^+ cells were sorted into FACS tubes with DMEM supplemented with 20% FBS and 1% antibiotic-antimycotic solution. After sorting, cells were cultured until confluence.

Genomic DNA extraction, genotyping PCR, and sequencing

Genomic DNA from sorted and cultured wild-type and RFP^+ cells was extracted with the DNeasy Blood & Tissue kit (QIAGEN) according to the manufacturer's protocol. To detect donor integration into *AAVS1* locus, genomic DNA was amplified using Q5 Hot Start High-Fidelity Master Mix (New England Biolabs) with primers described in Table S1. PCR products were purified with the QIAquick PCR Purification Kit (QIAGEN) and sequenced.

Western blot analysis

The wild-type and RFP^+ cells were lysed in denaturing lysis buffer (50 mM Tris-HCl pH 7.5, 1% SDS, 5 mM EDTA, 10 mM β-mercaptoethanol [BME], 1 mM PMSF, and 15 U/mL DNase) in the presence of protease/phosphatase inhibitor cocktails (Thermo Scientific) and mixed by vortexing for 3 s at maximum speed, and samples were heated at 95°C for 5 min. Suspension was then diluted in NP-40 lysis buffer (50 mM Tris-HCl pH 7.4, 150 mM NaCl, 1% NP-40, and 5 mM EDTA) and mixed gently. The lysed suspension was passed through a 26-gauge needle attached to a 1-mL syringe and incubated on ice for 5 min. Samples were centrifuged for 15 min at 16,000 × *g* at 4°C. The supernatants were transferred to a fresh microcentrifuge tube, and protein concentrations were determined with a BCA Protein Assay Kit (Pierce, Thermo Scientific). 40 μg of total protein was boiled at 95°C for 5 min and loaded into SDS-PAGE gels (Bio-Rad) and then transferred to polyvinylidene fluoride (PVDF) membranes (Bio-Rad). Membrane was incubated with anti-uricase (sc-166070, Santa Cruz Biotechnology) or anti-catalase (#21260-1-AP, Proteintech-Thermo Scientific) or anti-b-actin (sc-47778, Santa Cruz Biotechnology). Membranes were incubated with horseradish peroxidase (HRP)-conjugated secondary antibodies. Signal was detected after incubation with a Clarity Western ECL Substrate kit (Bio-Rad) and recorded with a ChemiDoc Imaging System (Bio-Rad).

Immunofluorescence and confocal microscopy

HEK293 RFP^+ and control wild-type cells were cultured under glass coverslips in 24-well plates (5×10^4). To determine the colocalization of peroxisomes and AncUOX, cells were fixed, permeabilized, blocked, and stained with anti-peroxisomal membrane protein 70 (PMP70), using the SelectFX Alexa Fluor 488 Peroxisome Labeling Kit (Invitrogen, Molecular Probes) according to the manufacturer's instructions. Cells were rinsed and then stained with anti-uricase (sc-166070, Santa Cruz Biotechnology) and secondary anti-mouse Alexa Fluor 647 (Thermo Fisher). Nuclei were stained with DAPI. Images were captured with a 63× oil immersion objective by using a LSM 700 laser scanning confocal microscope (Zeiss).

Uricase activity

Uricase activity was measured by monitoring the decrease of absorbance at 293 nm due to the enzymatic oxidation of uric acid. 1 mM uric acid stock solution was freshly prepared in 0.1 M sodium phosphate buffer, pH 7.4, and the solution was incubated at 37°C for 5 min with shaking. The assays were performed in triplicate with the following uric acid concentrations: 100 μM, 200 μM, 400 μM, and 600 μM diluted in 0.1 M sodium phosphate buffer, pH 7.4. Uric acid solutions were microscopically analyzed to confirm the absence of substantial uric acid crystallization. Cells were lysed with 1× Assay Buffer Uric Acid/Uricase Assay Kit (Cell Biolabs). Data were normalized by total protein concentration.

SUPPLEMENTAL INFORMATION

Supplemental information can be found online at https://doi.org/10.1016/j.omtn.2021.08.002.

ACKNOWLEDGMENTS

This work was supported by NIH Grant R01AR069137, Human Frontier Science Program Grant RGP0041, and Department of Defense Grant MURI W911NF-16-1-0372. We thank Ze Lake Li, Lily Tran, Elizabeth Slack, and Caden Gaucher for the assistance with experiments.

AUTHOR CONTRIBUTIONS

L.d.L.B. and E.A.G. conceived the study, analyzed data, and wrote the manuscript. L.d.L.B. conducted the experiments.

DECLARATION OF INTERESTS

E.A.G. is the owner of General Genomics, LLC, which has licensed the ancient uricase used in the present study.

REFERENCES

1. Ames, B.N., Cathcart, R., Schwiers, E., and Hochstein, P. (1981). Uric acid provides an antioxidant defense in humans against oxidant- and radical-caused aging and cancer: a hypothesis. Proc. Natl. Acad. Sci. USA *78*, 6858–6862.

2. Hershfield, M.S., Roberts, L.J., 2nd, Ganson, N.J., Kelly, S.J., Santisteban, I., Scarlett, E., Jaggers, D., and Sundy, J.S. (2010). Treating gout with pegloticase, a PEGylated urate oxidase, provides insight into the importance of uric acid as an antioxidant in vivo. Proc. Natl. Acad. Sci. USA *107*, 14351–14356.

3. Wu, X.W., Muzny, D.M., Lee, C.C., and Caskey, C.T. (1992). Two independent mutational events in the loss of urate oxidase during hominoid evolution. J. Mol. Evol. *34*, 78–84.

4. Kratzer, J.T., Lanaspa, M.A., Murphy, M.N., Cicerchi, C., Graves, C.L., Tipton, P.A., Ortlund, E.A., Johnson, R.J., and Gaucher, E.A. (2014). Evolutionary history and

metabolic insights of ancient mammalian uricases. Proc. Natl. Acad. Sci. USA *111*, 3763–3768.

5. Johnson, R.J., Gaucher, E.A., Sautin, Y.Y., Henderson, G.N., Angerhofer, A.J., and Benner, S.A. (2008). The planetary biology of ascorbate and uric acid and their relationship with the epidemic of obesity and cardiovascular disease. Med. Hypotheses *71*, 22–31.
6. Johnson, R.J., Stenvinkel, P., Andrews, P., Sánchez-Lozada, L.G., Nakagawa, T., Gaucher, E., Andres-Hernando, A., Rodriguez-Iturbe, B., Jimenez, C.R., Garcia, G., et al. (2020). Fructose metabolism as a common evolutionary pathway of survival associated with climate change, food shortage and droughts. J. Intern. Med. *287*, 252–262.
7. Cicerchi, C., Li, N., Kratzer, J., Garcia, G., Roncal-Jimenez, C.A., Tanabe, K., Hunter, B., Rivard, C.J., Sautin, Y.Y., Gaucher, E.A., et al. (2014). Uric acid-dependent inhibition of AMP kinase induces hepatic glucose production in diabetes and starvation: evolutionary implications of the uricase loss in hominids. FASEB J. *28*, 3339–3350.
8. Johnson, R.J., Lanaspa, M.A., and Gaucher, E.A. (2011). Uric acid: a danger signal from the RNA world that may have a role in the epidemic of obesity, metabolic syndrome, and cardiorenal disease: evolutionary considerations. Semin. Nephrol. *31*, 394–399.
9. Tan, P.K., Farrar, J.E., Gaucher, E.A., and Miner, J.N. (2016). Coevolution of URAT1 and Uricase during Primate Evolution: Implications for Serum Urate Homeostasis and Gout. Mol. Biol. Evol. *33*, 2193–2200.
10. Johnson, R.J., Sautin, Y.Y., Oliver, W.J., Roncal, C., Mu, W., Gabriela Sanchez-Lozada, L., Rodriguez-Iturbe, B., Nakagawa, T., and Benner, S.A. (2009). Lessons from comparative physiology: could uric acid represent a physiologic alarm signal gone awry in western society? J. Comp. Physiol. B *179*, 67–76.
11. Feig, D.I., Kang, D.H., and Johnson, R.J. (2008). Uric acid and cardiovascular risk. N. Engl. J. Med *359*, 1811–1821.
12. Perez-Ruiz, F., Calabozo, M., Fernandez-Lopez, M.J., Herrero-Beites, A., Ruiz-Lucea, E., Garcia-Erauskin, G., Duruelo, J., and Alonso-Ruiz, A. (1999). Treatment of chronic gout in patients with renal function impairment: an open, randomized, actively controlled study. J. Clin. Rheumatol. *5*, 49–55.
13. Goldman, S.C., Holcenberg, J.S., Finklestein, J.Z., Hutchinson, R., Kreissman, S., Johnson, F.L., Tou, C., Harvey, E., Morris, E., and Cairo, M.S. (2001). A randomized comparison between rasburicase and allopurinol in children with lymphoma or leukemia at high risk for tumor lysis. Blood *97*, 2998–3003.
14. Sundy, J.S., Baraf, H.S., Yood, R.A., Edwards, N.L., Gutierrez-Urena, S.R., Treadwell, E.L., Vazquez-Mellado, J., White, W.B., Lipsky, P.E., Horowitz, Z., Huang, W., et al. (2011). Efficacy and tolerability of pegloticase for the treatment of chronic gout in patients refractory to conventional treatment: two randomized controlled trials. JAMA *306*, 711–720.
15. Lyseng-Williamson, K.A. (2011). Pegloticase: in treatment-refractory chronic gout. Drugs *71*, 2179–2192.
16. Lipsky, P.E., Calabrese, L.H., Kavanaugh, A., Sundy, J.S., Wright, D., Wolfson, M., and Becker, M.A. (2014). Pegloticase immunogenicity: the relationship between efficacy and antibody development in patients treated for refractory chronic gout. Arthritis Res. Ther. *16*, R60.
17. Zhou, Y., Zhang, M., He, D., Hu, X., Xiong, H., Wu, J., Zhu, B., and Zhang, J. (2016). Uricase alkaline enzymosomes with enhanced stabilities and anti-hyperuricemia effects induced by favorable microenvironmental changes. Sci. Rep. *7*, 20136.
18. Jung, S., and Kwon, I. (2017). Synergistic Degradation of a Hyperuricemia-Causing Metabolite Using One-Pot Enzyme-Nanozyme Cascade Reactions. Sci. Rep. *7*, 44330.
19. Browning, L.A., and Kruse, J.A. (2005). Hemolysis and methemoglobinemia secondary to rasburicase administration. Ann. Pharmacother. *39*, 1932–1935.
20. Sadelain, M., Papapetrou, E.P., and Bushman, F.D. (2011). Safe harbours for the integration of new DNA in the human genome. Nat. Rev. Cancer *12*, 51–58.
21. Oceguera-Yanez, F., Kim, S.I., Matsumoto, T., Tan, G.W., Xiang, L., Hatani, T., Kondo, T., Ikeya, M., Yoshida, Y., Inoue, H., and Woltjen, K. (2016). Engineering the AAVS1 locus for consistent and scalable transgene expression in human iPSCs and their differentiated derivatives. Methods *101*, 43–55.
22. Chu, V.T., Weber, T., Wefers, B., Wurst, W., Sander, S., Rajewsky, K., and Kühn, R. (2015). Increasing the efficiency of homology-directed repair for CRISPR-Cas9-induced precise gene editing in mammalian cells. Nat. Biotechnol. *33*, 543–548.
23. Cheng, C.Y., Gilson, T., Dallaire, F., Ketner, G., Branton, P.E., and Blanchette, P. (2011). The E4orf6/E1B55K E3 ubiquitin ligase complexes of human adenoviruses exhibit heterogeneity in composition and substrate specificity. J. Virol. *85*, 765–775.
24. Forrester, N.A., Sedgwick, G.G., Thomas, A., Blackford, A.N., Speiseder, T., Dobner, T., Byrd, P.J., Stewart, G.S., Turnell, A.S., and Grand, R.J. (2011). Serotype-specific inactivation of the cellular DNA damage response during adenovirus infection. J. Virol. *85*, 2201–2211.
25. Pierzynowska, K., Deshpande, A., Mosiichuk, N., Terkeltaub, R., Szczurek, P., Salido, E., Pierzynowski, S., and Grujic, D. (2020). Oral Treatment With an Engineered Uricase, ALLN-346, Reduces Hyperuricemia, and Uricosuria in Urate Oxidase-Deficient Mice. Front. Med. (Lausanne) *7*, 569215.
26. Farina, B., Faraone Mennella, M.R., and Leone, E. (1979). Main properties of ox kidney uricase. Ital. J. Biochem. *28*, 270–279.
27. Truszkowski, R., and Gubermanówna, S. (1935). Uricase and its action: Extraction and precipitation of ox kidney uricase. Biochem. J. *29*, 2787–2797.
28. Vargas-Santos, A.B., and Neogi, T. (2017). Management of Gout and Hyperuricemia in CKD. Am. J. Kidney Dis. *70*, 422–439.
29. Ouchi, R., Togo, S., Kimura, M., Shinozawa, T., Koido, M., Koike, H., Thompson, W., Karns, R.A., Mayhew, C.N., McGrath, P.S., et al. (2019). Modeling Steatohepatitis in Humans with Pluripotent Stem Cell-Derived Organoids. Cell Metab. *30*, 374–384.e6.
30. Prior, N., Inacio, P., and Huch, M. (2019). Liver organoids: from basic research to therapeutic applications. Gut *68*, 2228–2237.
31. Collin de l'Hortet, A., Takeishi, K., Guzman-Lepe, J., Morita, K., Achreja, A., Popovic, B., Wang, Y., Handa, K., Mittal, A., Meurs, N., et al. (2019). Generation of Human Fatty Livers Using Custom-Engineered Induced Pluripotent Stem Cells with Modifiable SIRT1 Metabolism. Cell Metab. *30*, 385–401.e9.
32. Zakas, P.M., Coyle, C.W., Brehm, A., Bayer, M., Solecka-Witulska, B., Radford, C.E., Brown, C., Nesbitt, K., Dwyer, C., Kannicht, C., et al. (2021). Molecular coevolution of coagulation factor VIII and von Willebrand factor. Blood Adv. *5*, 812–822.
33. Zakas, P.M., Brown, H.C., Knight, K., Meeks, S.L., Spencer, H.T., Gaucher, E.A., and Doering, C.B. (2017). Enhancing the pharmaceutical properties of protein drugs by ancestral sequence reconstruction. Nat. Biotechnol. *35*, 35–37.
34. Selberg, A.G.A., Gaucher, E.A., and Liberles, D.A. (2021). Ancestral Sequence Reconstruction: From Chemical Paleogenetics to Maximum Likelihood Algorithms and Beyond. J. Mol. Evol. *89*, 157–164.
35. Gumulya, Y., and Gillam, E.M. (2017). Exploring the past and the future of protein evolution with ancestral sequence reconstruction: the 'retro' approach to protein engineering. Biochem. J. *474*, 1–19.
36. Johnson, R.J., and Andrews, P. (2010). Fructose, Uricase, and the Back-to-Africa Hypothesis. Evol. Anthropol. *19*, 250–257. https://doi.org/10.1002/Evan.20266.
37. Johnson, R.J., Perez-Pozo, S.E., Sautin, Y.Y., Manitius, J., Sanchez-Lozada, L.G., Feig, D.I., Shafiu, M., Segal, M., Glassock, R.J., Shimada, M., Roncal, C., et al. (2009). Hypothesis: could excessive fructose intake and uric acid cause type 2 diabetes? Endocr. Rev *30*, 96–116.
38. Ran, F.A., Hsu, P.D., Wright, J., Agarwala, V., Scott, D.A., and Zhang, F. (2013). Genome engineering using the CRISPR-Cas9 system. Nat. Protoc. *8*, 2281–2308.